Military Technical College
Kobry El-Kobbah,
Cairo, Egypt

8th International Conferenc
on
Chemical & Environmenta
Engineering
19 – 21 April 2016

PCEA -2

Preparation and Characterization of PANI/TiO_2 Composite for Photocatalytic Degradation of Tartrazine Dye

Mohamed Gobara* and M. A. Elsayed*

Abstract

HCl-doped polyaniline (PANI) and composites of polyaniline and titanium dioxide (PANI/ TiO_2) with different PANI:TiO_2 ratios were chemically prepared. The mechanism of preparation of the composite suggested that the aniline was adsorbed on the TiO_2 surface before polymerization process took places. PANI and PANI/ TiO_2 are characterized using FTIR, SEM, EDX and XRD. The results showed that, the prepared PANI was emelardine salt and has an amorphous structure. The thermal stability of prepared samples was characterized using thermo gravimetric (TG) analysis. PANI is stable up to 200 °C and the relative weights percent of PANI in the PANI/TiO_2 composite were 20, 25, 40 and 45 percent for the prepared samples. Photocatalytic activity of PANI/TiO_2 composite via Tatrazine (TZ) azo dye was investigated under UV light irradiations and compared with unmodified PANI and TiO_2 particles. Results indicated the superiority of the prepared composite photo-catalyst over pure PANI and TiO_2. However, the excessive PANI percent tends to form a relatively thick layer and even aggregate on the surface of TiO_2. This hinders the migration of excited electrons from the outer PANI layer to the inner TiO_2 particles, which consequently leads to decrease the degradation efficiency. A possible mechanism for the photocatalytic oxidative degradation was also mentioned.

Keywords: Photo-catalytic, PANI, TiO_2, Tartrazine, TG.

---

* Corresponding author Present address: Military Technical College, Kobbry Elkobba, Cairo, Egypt, Tel.: +20 1144 919 619, fax: +20 226 219 08
E-mail address: m_gobara@yahoo.com

Military Technical College
Kobry El-Kobbah,
Cairo, Egypt

8th International Conferenc
on
Chemical & Environmenta
Engineering
19 – 21 April 2016

1. Introduction

Interest in the study of conductive polymers has increased dramatically over the last 25 years as a result of the advantages of using conductive polymers, notably that they are light, inexpensive and easily processed. The electrical conductivity of these polymers is considered to be intermediate between insulators and metals; with a specific conductivity of range 10^9 - 10^6 S/cm [1].

Polyaniline is one of the oldest known synthetic organic conductive polymers. In 1862 Letheby obtained a partly conductive material which was polyaniline by anodic oxidation of aniline in sulphuric acid [2]. Polyaniline take great interest during last decade. This interest is caused by the unique properties of PANI; notably that it is relatively cheap, easy to synthesize and very stable under a wide variety of experimental conditions. The electrical and optical behaviour of these forms are strongly dependent on pH and dopant effects [3, 4]. Polyaniline has been used in many applications; including rechargeable batteries, electrochromic display devices, intelligent windows, transparent electrode, electromagnetic impulse shielding, sensors, gas separation membranes, solar cells, fuel cells, corrosion protection, printed circuit boards, biomedical applications and transparent conductive coatings [5-10].
Polyaniline (PANI), with an extended conjugated electron system, shows considerable absorption coefficients in the visible-light range with high mobility of charge carriers [11]. Chemical structure of polyaniline salts can be simply shown in Figure 1.

TiO_2 is one of the typical of n-type semiconductor which produces electron-hole pairs under illumination of UV light. TiO_2 photo-catalyst has been successfully used to decontaminate wastewaters and to degrade the organic pollutants [12]. Owing to rather high intrinsic band gap of TiO_2 (3.2 eV for anatase) only about 4% of the solar energy can be utilized. The photocatalytic activity of TiO_2 is governed by various factors such as surface area, phase structure, interfacial charge transfer, and the separation efficiency of photo-induced electrons and holes. However, the poor within the visible-light spectral range limits the uses of TiO_2 materials. In addition, there exists a high rate of electron–hole recombination which limits redox applications [13].

Regarding the efficient carrier-transfer property of PANI, it is expected that coupling of PANI with TiO_2 would enhance the photocatalytic activity under UV light. Recently, some studies have reported on the combination of PANI and TiO_2 with the aim of improving their photocatalytic performance when exposed to UV light or sunlight. However, as reported, most of photocatalysts were coupled with PANI through a simple dipping procedure [14].

Various research works have been carried out to make TiO_2 photocatalysts efficient harvesting visible light by dye sensitization, polymer modification, non-metals doping, semiconductor coupling, transition metal doping, and spatial structuring[13, 15-17]

Dyes as, coloring agents, are released from different sources such as food and textile industries. They are considered to be one of the largest contributors of environment pollution and some are toxic and/or carcinogenic in nature. In addition, the colored aqueous effluents released in water bodies reduce the penetration of light which leads to reduction in the rate of photosynthesis of the dyes. This decreases the amount of dissolved oxygen which ultimately is essential for the survival of aquatic species[18].

Complete mineralize of organic pollutants is important for wastewater remediation and advanced oxidation process (AOP), particularly when using photo-catalysis, has the capability to achieve this aim. Accordingly, it is considered more efficient remediation method than the conventional dye removal methods [19].

The present work introduces the synthesis of PANI/TiO_2 composites with different PANI weight ratios where the prepared samples were characterized by FTIR, XRD and SEM. The photocatalytic degradation of Tatrazine (TZ) dye under the ambient air atmosphere was investigated using the prepared samples. The effect of PANI to TiO_2 ratio on the photocatalytic process was also investigated.

2. Experimental

All chemicals were purchased from Sigma-Aldrich and were used as received except aniline; it was double distilled with a zinc powder before polymerization.

2.1 Samples preparation and characterizations

Polyaniline was prepared employing chemical oxidation of double distilled aniline by ammonium persulphate in HCl solution (1 M). In brief, double distilled aniline (5.0 ml) was dissolved in HCl (300 ml, 1 M) at 0-5ºC and stirred for 1 hour. Ammonium persulphate (5.6 g) was dissolved in HCl (100 ml, 1M) and was added drop-wise to aniline solution over a period of 15 minutes with vigorous stirring. The mixture solution was then continually stirred overnight at 0-5ºC. The produced PANI precipitate was collected with a Buchner funnel and washed with ethanol to remove any oligomers and then was washed with four portions of HCl (50 ml, 1 M). The precipitate was dried at 60ºC for 24 hours and the pure HCl-doped PANI (emeraldine salt, ES) was obtained as a green powder. The powder was then grinded and refined using ball mill.

Titanium dioxide was prepared by hydrolysis and condensation of titanium tetra isopropoxide (TTIP). TTIP (5 ml) was dissolved in iso-propanol (10 ml). Nitric acid (0.01 M) was then added drop-wise to TTIP solution with vigorous stirring till reaching pH of 1.5. Stirring continued for 24 hours where the homogenous transparent TiO_2 sol was obtained. The sol was dried in microwave for 15 minutes to obtain TiO_2 powder. The powder was then calcinated at 450°C for 4 hours to obtain the desired TiO_2 particles.

Military Technical College
Kobry El-Kobbah,
Cairo, Egypt

I.C.E.E.2016

8th International Conferenc on Chemical & Environmenta Engineering
19 – 21 April 2016

PANI/TiO_2 composite samples were prepared with different organic/inorganic (PANI-TiO_2) weight ratios. The samples were signed as PT-1, PT-2 and PT-3. Typically for each sample, TiO_2 powder (2 g) was added to a specified amount of cooled (0-5ºC) and stirred (for 8 hours) acidic solution of double distilled aniline (1, 2 and 3 ml for PT-1, PT-2 and PT-3 composite samples, respectively). The polymerization of aniline for these samples was performed in the same manner as discussed above. The collected precipitates were pale green powder of the PANI/TiO_2 composites. Figure 2 illustrates the formation mechanism of PANI/TiO_2 composite. In which, TiO_2 particles are positively charged in acidic solution, required for the in-situ polymerization of aniline. Chloride anions are adsorbed on the positively charged surface of TiO_2 nanoparticles to neutralize the created positive charge on the surface of TiO_2 nanoparticles. Aniline monomer in acidic solution (HCl) is transformed to the anilinium cation. Therefore, electrostatic interaction occurred between chloride anions adsorbed on the surface of TiO_2 nanoparticles and anilinium monomers, which are available in reaction media. Polymerization of anilinium cations, causes formation of PANI-TiO_2 composite.
Another sample was also prepared by just through mechanical mixing of powders of PANI and TiO_2 (PT-mix).

Surface characterization of the prepared samples was performed by SEM using the fully computerized Philips XL 40 microscope equipped with energy dispersive X-ray analysis. Chemical structure was investigated by IR analysis of the prepared samples using FTIR Jasco-4100. The spectra in the fingerprint range of 400–1600 cm^{-1} with automatic signal gain of 128 scans at 4 cm^{-1} resolution. The background spectrum was recorded from the clean empty cell at 25°C and was taken in consideration during analysis of all samples. Thermal Gravimetric Analysis (TGA) was carried out using Rigaku Thermal Analyzer instrument. The analyses were performed using 10 mg of each sample which was heated from room temperature to 700°C with heating rate of 10°C/min.

2.2 Evaluation of photo-catalysis

The photocatalytic activity of PANI, TiO_2, (PT-1) and (PT-mix) were evaluated by determining the removal efficiency and rate constant of TZ photo-degradation. The aqueous solutions of TZ were used as model pollutant for investigation of the photocatalytic activity of samples. TZ aqueous solutions (100 ml each) were treated by calculated amounts of PANI, TiO_2, PT-1 and PT-mix (5 mg). Afterward, the suspensions were illuminated by a 10 W low-pressure mercury lamp (90% emittance at 254 nm) located axially with treated solution vials. At time intervals, liquors from the vials (3 ml) were withdrawn by a syringe equipped with 2.5 μm pore size for recording absorbance at λ_{max}(TZ) = 425 nm with a UV-Vis spectrophotometer. The remaining concentrations, with time, of TZ were calculated using the standard calibration curve (Figure 3). Calibration curve was determined from UV-Vis absorption spectra of different concentrations of TZ aqueous solutions, Figure 4. The photocatalytic degradation efficiency was calculated according to the following equation:

Military Technical College
Kobry El-Kobbah,
Cairo, Egypt

I.C.E.E.2016

8th International Conferenc
on
Chemical & Environmenta
Engineering
19 – 21 April 2016

$$\text{Removal efficiency} = [(C_o - C_t)/ C_o] \times 100 \quad (1)$$

Where C_o is the initial concentration of Tartrazine (TZ) and C_t is the solution concentration after photocatalytic degradation at any time.

3. Results and discussions

3.1. Sample characterization

Figure. 5a shows the IR spectrum of TiO_2. The sharp peak at 501cm^{-1} refers to the Ti–O bond. The narrow bands at 1618 and 1141 cm^{-1} refer to the residues of organic precursors of preparation procedure. The other peaks are due to absorbed organic molecules on the surface of TiO_2 particles.

Figure 5b shows the IR spectrum of the prepared polyaniline (PANI). The spectrum consists of five main peaks at 809, 1149, 1300, 1486, and 1585 cm^{-1}. These peaks represent bending vibration of C−H on the aromatic rings, vibration of N=Q=N ring, stretching vibration of C−N, stretching vibration of N−B−N ring and stretching vibration of N=Q=N rings, respectively (Q is the quinone ring and B is the benzene ring). This result agrees with previous IR analysis of PANI [16, 20]. The spectrum shows that peaks at 1486 and 1585 cm^{-1} are of comparable heights which suggests that this polymer is in its conductive oxidation state (emeraldine salt) [15].

Figure 5c shows the IR spectrum of the prepared PANI/TiO_2 composite (PT-1). In the range 1000 - 2000 cm^{-1}, the spectrum is almost similar to that of PANI and no new peaks can be observed. In the range 400 - 1000 cm^{-1}, the spectrum is apparently the sum of that of PANI and TiO_2, however, the peak of TiO_2 at 501 cm^{-1} is slightly shifted to a lower wave number , 433 cm^{-1}, indicating physical adsorption of aniline on the TiO_2 surface during preparation process [21]. Meanwhile, the characteristic peak of N-H stretching mode at 3457 cm^{-1} of PANI shifted to a lower wavenumber (3432 cm^{-1}) in the PANI-TiO2 composite, and the hydrogen bond absorption at 3230 cm^{-1} is strengthened after TiO_2 was introduced. These findings reveal that the hydrogen bonding in the PANI complex became stronger after complexing with TiO_2. The results also suggest that there is strong interaction between the polyaniline and TiO_2 [15].

Figure 6(a) shows the XRD pattern of the prepared TiO_2 with peaks positioned at (2θ) = 26, 38, 48, 54, 62 and 70. This pattern confirms the formation of anatase phase with few rutile percentage appeared at positions (2θ) = 28, 32, 37 and 42 [22]. The XRD software calculated weight percent of anatase and rutile phases are 80% and 20 % respectively.

Military Technical College
Kobry El-Kobbah,
Cairo, Egypt

I.C.E.E.2016

8th International Conferenc on Chemical & Environmenta Engineering
19 – 21 April 2016

Figure 6(b) shows the XRD pattern of the prepared PANI. The pattern is broad peak which reflects the amorphous nature of the prepared PANI. The main broad peaks present at 2θ = 19.9 and 25.4. However, few studies mention the peak located at 2θ = 16 and 6.2 [23, 24]. The appearance of these XRD peaks depends on the polyaniline synthesis conditions that interfere in their physical and chemical characteristics.
Figure 6(c) shows the XRD pattern of the prepared PT-1 composite sample. The pattern is almost similar to that of the TiO_2. This indicates that the crystal structure of the TiO_2 particles is not customized by the presence of PANI in the composites. Furthermore, these results confirm the amorphous nature of PANI in the composites, suggesting that the addition of TiO_2 particles restrain the amorphous nature of the PANI molecular chains.

The SEM image of the PT-1 composite is shown in Figure 7 where it can be observed the titanium particles (white spots) are surrounded by the PANI polymer which seems to be in a sponge shape. This confirms the amorphous structure of PANI. Moreover, EDX analysis of the points 1 and 2 in Figure 7 are shown in Figure 8(a) and (b), respectively where both confirm the presence and good distribution of TiO_2 particles within the matrix of PANI polymer. These results are in agreement with the above postulated mechanism of preparation of PANI /TiO_2 composite.

a

3.2 Thermal gravimetric analysis

Before investigating the photo-catalyst activity of prepared samples, the PANI to TiO_2 weight ratio of the prepared composite ought to be studied. Thermal gravimetric (TG) analysis was exploited in this study to calculate this weight ratio.

b

Figure 9 shows the thermograms of PANI, TiO_2 and PT-1 samples. TiO_2 sample shows weight loss of 2.5% from 30-120°C and it has become of stable weight till the end of the test. This weight loss may be due to the evaporation of moisture content. PANI sample shows weight loss in three steps with a continuous weight loss mode; first step from 30-120°C which may relate to the evaporation of ethanol, moisture and physi-sorbed water molecules collected during preparation procedure with a total weight loss of ca. 11% [25, 26]. Second step from 150-220°C which may relate to the broken down of Cl^- from the backbone of the polymer and crosslinking reaction of two neighboring –N=Q=N– groups producing –N–B–H– groups through linking of nitrogen atom with its neighboring quinoid ring [11, 26]. During the last step (300-610°C), the polymer begins to have a skeletal degradation of polymer chain structure that completely decomposes at ca. 600°C [12, 27] and the sample loosed about 72% of its original weight with residual inorganic impurities of about 3%. This result confirms the good thermal stability of polyaniline below 200°C temperature.

c

The PT-1 shows a continuous weight loss from room temperature up to 630°C with a total weight loss of 23% due to evaporation of solvent and moisture and decomposition of polyaniline content. The sample weight loss is ≈ 3% up to 120°C and the rest of the 23% is

lost from 120 to 630°C. From the above results, it can conclude that the PANI content (in wt%) in the PT-1 is (19.6) ≈ 20% and hence TiO_2 content is 80%. The same procedures have been applied to the other prepared samples and Table (1) shows the weight ratio of the PANI to TiO_2 for the prepared samples; PT-1, PT-2, PT-3, PT-4.

Table (1) the weight ratio of the PANI to TiO_2 in the PANI/TiO_2 composite samples from thermal gravimetric analysis

Sample code	PANI Weight percent (%)	TiO_2 Weight percent (%)
PT-1	19.6	80.4
PT-2	26.1	73.9
PT-3	40.3	59.7

3.3 Photocatalytic activities study

In this part of work, the percent removal of TZ by PANI, TiO_2, and PT-1 composite coupled with UV light irradiations was evaluated. To study the synergistic effect between PANI and TiO_2, the amount of PANI used in this experiment is the same as in PT-1 and the amount of TiO_2 is also the same amount in the PT-1. In addition, a new sample (PT-mix) was introduced in this part of study. The PT-mix represents the mechanical mixture of PANI and TiO_2 with the same weight percent of PT-1. This sample was used to clarify the effect of presence of PANI on the surface of TiO_2 of PT-1 sample rather than to exist in the solution of photocatalytic.

The photocatalytic degradation efficiency was obtained according to the procedure described in section 2.2. Figure 10 shows that photo-degradation efficiency of TZ using PT-1 composite is significantly higher than other samples. PANI/TiO_2 composite photo-catalytically degraded about 99% of TZ as compared to only about 40% by pure Titania in 120 minutes. This clearly suggests the superiority of the prepared composite photo-catalyst over the pure TiO_2. This can be attributed to the efficient charge separation of photo-generated electrons and holes when coupling the conductive polymer (PANI) and the semiconductor (TiO_2).

On the other hand, one of the possible reasons for the improvement of PANI/TiO_2 photo-catalytic activity under UV light illuminations is the reduced aggregation state of TiO_2 particles in PANI/TiO_2 composite. This leads to the higher specific surface area and higher interaction between PANI/TiO2 photocatalyst and dye aqueous solution compared to pristine TiO_2 particles [28]. Therefore, adsorption of dye molecules on the composite is higher than pristine TiO_2 particles.

Wang et al., (2014) found that, the PANI/TiO_2 nanocomposite exhibits different optical behaviour from that observed for pristine TiO_2 nanoparticles. PANI/TiO_2 nanocomposite not only absorbs the UV light but also significantly absorb the visible and near-IR. Whereas pristine TiO_2 nanoparticles absorb only the UV region and a small part of visible light. These results indicate that PANI is a good sensitizer for TiO_2 nanoparticles and increases the photoactive region of TiO_2 nanoparticles through the absorption of visible and near-IR lights [29]

To investigate the effect of the adsorption process, the experiments were repeated under dark condition and the results were shown in Figure 11. As can be seen in Figure 11, the removal percentages of TZ due to adsorption mechanism under dark condition are about 2%, 7%, 9% and 15% in the presence of the TiO_2, PANI, PT-mix and the PT-1 composite, respectively. The de-colorization efficiencies of TZ are very higher than corresponding dark conditions in the presence of the PANI/TiO_2 composite under UV-illumination. The results show that the PANI/TiO_2 composite exhibit good photocatalytic performance.

The above results show that photo-degradation mechanism governed the de-colorization process in all the samples containing TiO_2. Moreover, the total removal of TZ with sample PT-mix is 53% which is slightly higher than the sum of both adsorption of PANI sample (9%) and photo-degradation of TiO_2 (40%). These results indicate that the mechanical mixture of PANI and TiO_2 has a limited synergistic effect on the overall photocatalytic process. However, in the case of PT-1 the removal of TZ is significantly greater (99%) than the sum of photo-degradation and adsorption. This clarifies the synergistic effect of presence of PANI on the surface of TiO_2 on photo degradation process.

The kinetic plots (Figure 12) for TZ degradation with PANI, TiO_2, PT-mix and PT-1 composite photocatalysts under UV illumination are shown by pseudo-first order reaction [30]. This model is described by equation (2).

$$-\ln (C_t/C_o) = k_{app}\, t \qquad (2)$$

Where k_{app} is the apparent rate constant, C_o is the initial concentration of TZ and C_t is the concentration of TZ at various contact times, *t*.

Half time of TZ photo-degradation was calculated using equation (3) which was derived from equation (2) by replacing C_t by $C_o/2$:

$$T_{1/2} = 0{\cdot}6931/k_{app} \qquad (3)$$

The determined pseudo-first-order rate constants (k_{app}), linear regression coefficients (R^2), degradation efficiency and half time of TZ photo-degradation after 170 min illumination are presented in Table 2. From Table 2, it can be seen that, the degradation efficiency of the

Military Technical College
Kobry El-Kobbah,
Cairo, Egypt

8th International Conferenc
on
Chemical & Environmenta
Engineering
19 – 21 April 2016

PANI/TiO_2 mechanical mixture is approximately the sum of that PANI and TiO_2 alone. However, the deposition of PANI on the surface of TiO_2 particles extremely improves the degradation efficiency, apparent rate constant and half time of TZ degradation compared to other photocatalysts.

Table 2. Apparent rate constants (k_{app}), linear regression coefficients, half time of TZ photo-degradation from a plot of $-\ln (C_t / C_o) = k_{app}$ and degradation efficiency (%) of TZ after 170 minutes of illumination under UV light.

Photocatalyst	Degradation Efficiency (%)	R^2	$k_{app}(min^{-1})$	$T_{1/2}$(min)
PANI	9	0.98	0.0005	1386.2
TiO_2	41.2	0.97	0.002	346.5
PANI/TiO_2 mechanical mix.	54.8	0.93	0.003	34.6
PANI/TiO_2 composite	99.1	0.95	0.029	23.9

3.4 Photocatalytic degradation mechanism

Figure 13 shows the proposed mechanism of photo-degradation of TZ dye by PANI/TiO_2 composite photo-catalyst under UV light irradiation. Both PANI and TiO_2 particles absorb photons at their interface under irradiation. Since the conduction band (CB) of TiO_2 and lowest unoccupied molecular orbital (LUMO) of PANI are well matched for the charge transfer. Under UV light illumination photo-generated holes in the valiancy band (VB) of TiO_2 can be transferred directly to highest unoccupied molecular orbital (HOMO) of PANI, as the VB of TiO_2 matches well with the HOMO of PANI [28]. Subsequently the photo-generated electron–hole pairs in the PANI/TiO_2 photo-catalyst interface can be transferred to the surface, which reacts directly with water , adsorbed TZ molecules on the surface of PT-1 or indirectly decompose TZ dye through the production of $OH^{\cdot}$ radicals [15]. The following reactions illustrate the degradation process on the composite surface.

$$\text{PANI/TiO}_2 + h\nu \rightarrow \text{PANI/TiO}_2\ (e^-, h^+) \quad (4)$$

$$\text{PANI/TiO}_2\ (e^-) + O_2 \rightarrow \text{PANI/TiO}_2 + O_2^{\cdot -} \quad (5)$$

$$\text{PANI/TiO}_2\ (h^+) + H_2O \rightarrow \text{PANI/TiO}_2 + OH^{\cdot} \quad (6)$$

$$TZ + OH^{\cdot} \rightarrow \text{Degradation Products} \quad (7)$$

On the other hand, charge separation enhancement in PANI/TiO_2 composite interface causes improvement of photocatalytic activity of PT-1 under UV light illuminations. This enhancement of charge separation in the PT-1 is achieved, because PANI is an efficient electron donor and good hole transporter. These features of PANI lead to the effective separation of photo-generated electron–holes at the interface of PANI and TiO_2 in the composite[31, 32].

Military Technical College
Kobry El-Kobbah,
Cairo, Egypt

I.C.E.E.2016

8th International Conferenc on Chemical & Environmenta Engineering
19 – 21 April 2016

In short, under UV light illumination, the synergic effect of PANI causes rapid charge separation, slow charge recombination and thus an enhanced photo catalytic activity **(PCA) of** the prepared PANI/TiO_2 photocatalysts. The main oxidative species in the PANI/TiO_2 composite photocatalytic process, under UV light irradiations are oxygenous radicals (•O), hydroxyl radical, (•OH) and holes (h^+) which attack the TZ molecule leads to its degradation.

3.5 Effect of PANI/TiO_2 ratio on the degradation efficiency

Figure 14 shows the effect of PANI/TiO_2 ratio on the degradation efficiency. The result showed that further increasing of the amount of PANI in the PANI/TiO_2 composite from 19.6% to 40.3% samples PT-1 to PT-3 respectively, the degradation efficiency increases due to adsorption effects. However، a further increase of the amount of PANI leads to decreases the degradation (sample PT-4 ; PANI 61% and TiO_2 39%). The results can be ascribed to different transferring rates of the photo-induced carriers and recombination of electron-holes pairs when different amounts of PANI are coated. High amount of PANI loading prevents TiO_2 from absorbing visible light, thus causing a rapid decrease in irradiation passing through the reaction system [21]. When the amount of PANI surpasses the threshold value, the excessive PANI particles tend to form a relatively thick layer and even aggregate on the surface of TiO_2 , thus hindering the migration of excited electrons from the outer PANI layer to the inner TiO_2 particles. Consequently, the number of radicals decreases and the photo-degradation of the dye pollutant is thus affected [28]. Therefore, the amount of PANI loading should be adequately controlled.

4. Conclusions

PANI was chemically prepared on the prepared TiO_2 surface. FTIR analysis confirms the preparation of PANI and reveals that the PANI was in its conductive oxidation state (emelardine salt). The XRD revealed that PANI has an amorphous structure. In addition, XRD analysis showed that the TiO_2 is 80% anatase phase and 20% rutile phase. The SEM surface morphology confirms that PANI was prepared on TiO_2 surface and it has an amorphous phase. The TG analysis showed PANI was stable up to 200°C and the PANI percent in PANI/TiO_2 composite is 20%. The photo-degradation of Tartrazine (TZ) under UV irradiation showed that the PANI/TiO_2 composite photo-catalyst degraded ≈99% of the dye as compared to only about 40% by pure titania in 120 min. This clearly suggested the superiority of the prepared composite photo-catalyst over pure TiO_2. Also, the obtained regression coefficients suggest the kinetics equation of TZ photo-degradation under UV light illuminations well concisely follow the pseudo-first order reaction kinetics.

5- References

[1] Gulce, H., et al., Preparation of a New Polyaniline/CdO Nanocomposite and Investigation of Its Photocatalytic Activity: Comparative Study under UV Light and Natural Sunlight Irradiation. Industrial & Engineering Chemistry Research, 2013. 52(32): p. 10924-10934.

[2] Letheby, H., On the production of a blue substance by the electrolysis of sulphate of aniline. J. Chem. Soc., 1862. 15: p. 161-163.
[3] MacDiarmid, A.G. and A.J. Epstein, Secondary doping in polyaniline. Synthetic Metals, 1995. 69(1): p. 85-92.
[4] Somani, P.R., Organic and Organic–Inorganic Hybrid Electrochromic Materials and Devices. Optical Properties of Functional Polymers and Nano Engineering Applications, 2014. 1: p. 187.
[5] Akid, R., M. Gobara, and H. Wang, Corrosion protection performance of novel hybrid polyaniline/sol–gel coatings on an aluminium 2024 alloy in neutral, alkaline and acidic solutions. Electrochimica Acta, 2011. 56(5): p. 2483-2492.
[6] Meng, Z.-D., L. Zhu, and W.-C. Oh, Preparation and high visible-light-induced photocatalytic activity of CdSe and CdSe-C_{60} nanoparticles. Journal of Industrial and Engineering Chemistry, 2012. 18(6): p. 2004-2009.
[7] Mostafaei, A. and A. Zolriasatein, Synthesis and characterization of conducting polyaniline nanocomposites containing ZnO nanorods. Progress in Natural Science: Materials International, 2012. 22(4): p. 273-280.
[8] Stejskal, J., et al., Purification of a conducting polymer, polyaniline, for biomedical applications. Synthetic Metals, 2014. 195: p. 286-293.
[9] Ramphal, I.A. and M.E. Hagerman, Water Processable Laponite/Polyaniline/Graphene Oxide Nanocomposites for Energy Applications. Langmuir, 2015.
[10] Ravalli, A., et al., Polyaniline Modified Thin-film Array for Sensor Applications, in Sensors. 2015, Springer. p. 123-127.
[11] Scherr, E.M., et al., Polyaniline: Oriented films and fibers. Synthetic Metals, 1991. 41(1–2): p. 735-738.
[12] Li, X., et al., Surface properties of polyaniline/nano-TiO_2 composites. Applied Surface Science, 2004. 229(1): p. 395-401.
[13] Tseng, Y.-H. and B.-K. Huang, Photocatalytic Degradation of Using Ni-Containing TiO_2. International Journal of Photoenergy, 2012. 2012.
[14] Liao, G., et al., Photonic crystal coupled TiO_2/polymer hybrid for efficient photocatalysis under visible light irradiation. Environmental science & technology, 2010. 44(9): p. 3481-3485.
[15] Zhang, L., P. Liu, and Z. Su, Preparation of PANI–TiO_2 nanocomposites and their solid-phase photocatalytic degradation. Polymer Degradation and Stability, 2006. 91(9): p. 2213-2219.
[16] Singh, S., H. Mahalingam, and P.K. Singh, Polymer-supported titanium dioxide photocatalysts for environmental remediation: A review. Applied Catalysis A: General, 2013. 462: p. 178-195.
[17] Radoičić, M., et al., Improvements to the photocatalytic efficiency of polyaniline modified TiO_2 nanoparticles. Applied Catalysis B: Environmental, 2013. 136: p. 133-139.

[18] Haspulat, B., A. Gülce, and H. Gülce, Efficient photocatalytic decolorization of some textile dyes using Fe ions doped polyaniline film on ITO coated glass substrate. Journal of hazardous materials, 2013. 260: p. 518-526.
[19] Di Paola, A., et al., A survey of photocatalytic materials for environmental remediation. Journal of hazardous materials, 2012. 211: p. 3-29.
[20] Zeng, X.-R. and T.-M. Ko, Structures and properties of chemically reduced polyanilines. Polymer, 1998. 39(5): p. 1187-1195.
[21] Qiao, Y., et al., Nanostructured polyaniline/titanium dioxide composite anode for microbial fuel cells. Acs Nano, 2007. 2(1): p. 113-119.
[22] Nadeem, M., et al., Study of ethanol reactions on H_2 reduced Au/TiO_2 anatase and rutile: effect of metal loading on reaction selectivity. Catalysis, Structure & Reactivity, 2015.
[23] Bilal, S., et al., Synthesis and characterization of completely soluble and highly thermally stable PANI-DBSA salts. Synthetic Metals, 2012. 162(24): p. 2259-2266.
[24] Tantawy, H.R., et al., Comparison of electromagnetic shielding with polyaniline nanopowders produced in solvent-limited conditions. ACS applied materials & interfaces, 2013. 5(11): p. 4648-4658.
[25] Yelil Arasi, A., et al., The structural properties of Poly (aniline)—Analysis via FTIR spectroscopy. Spectrochimica Acta Part A: Molecular and Biomolecular Spectroscopy, 2009. 74(5): p. 1229-1234.
[26] Salem, M.A., A.F. Al-Ghonemiy, and A.B. Zaki, Photocatalytic degradation of Allura red and Quinoline yellow with Polyaniline/TiO $_2$ nanocomposite. Applied Catalysis B: Environmental, 2009. 91(1): p. 59-66.
[27] Pielichowski, K., Kinetic analysis of the thermal decomposition of polyaniline. Solid State Ionics, 1997. 104(1): p. 123-132.
[28] Li, X., et al., Preparation of polyaniline-modified TiO_2 nanoparticles and their photocatalytic activity under visible light illumination. Applied Catalysis B: Environmental, 2008. 81(3): p. 267-273.
[29] Wang, W., et al., Bi_2 WO_6/PANI: An efficient visible-light-induced photocatalytic composite. Catalysis Today, 2014. 224: p. 147-153.
[30] Ansari, R., Application of polyaniline and its composites for adsorption/recovery of chromium (VI) from aqueous solutions. Acta chimica slovenica, 2006. 53(1): p. 88.
[31] Huang, X., et al., Synthesis of polyaniline-modified $Fe_3O_4/SiO_2/TiO_2$ composite microspheres and their photocatalytic application. 2011.
[32] Liao, G., et al., Remarkable improvement of visible light photocatalysis with PANI modified core–shell mesoporous TiO $_2$ microspheres. Applied Catalysis B: Environmental, 2011. 102(1): p. 126-131.

Military Technical College
Kobry El-Kobbah,
Cairo, Egypt

I.C.E.E.2016

8th International Conferenc on Chemical & Environmenta Engineering
19 – 21 April 2016

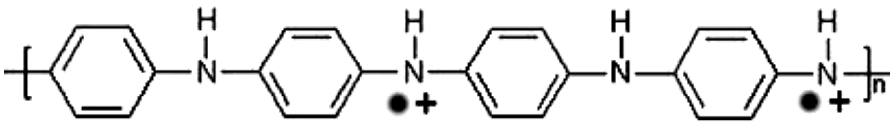

Figure 1. Chemical structure of acid doped polyaniline (Emeraldine salt)

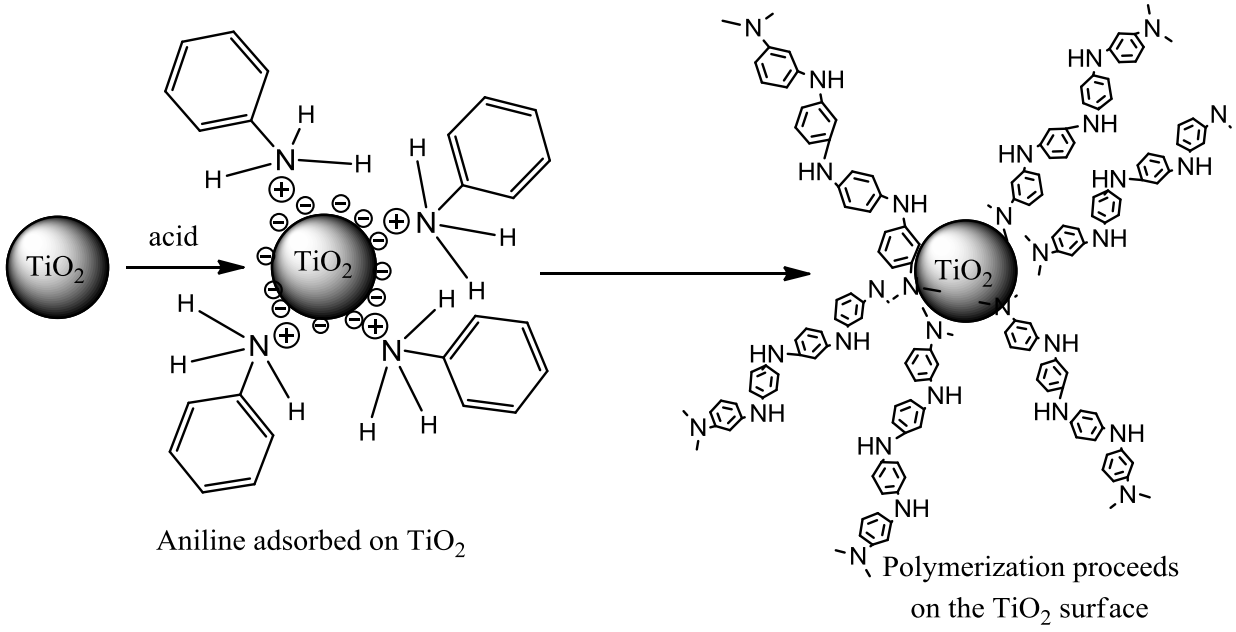

Figure 2 Formation scheme of PANI / TiO_2composite sample

Military Technical College
Kobry El-Kobbah,
Cairo, Egypt

I.C.E.E.2016

8th International Conferenc
on
Chemical & Environmenta
Engineering
19 – 21 April 2016

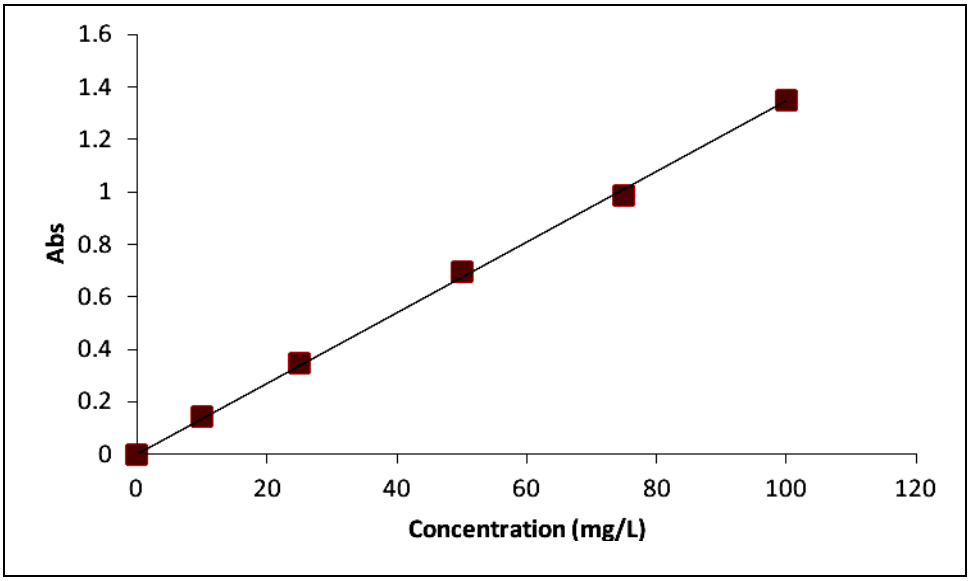

Figure 3 Calibration curve of Tartrazine at pH = 6.8 and λ_{max}= 425 nm.

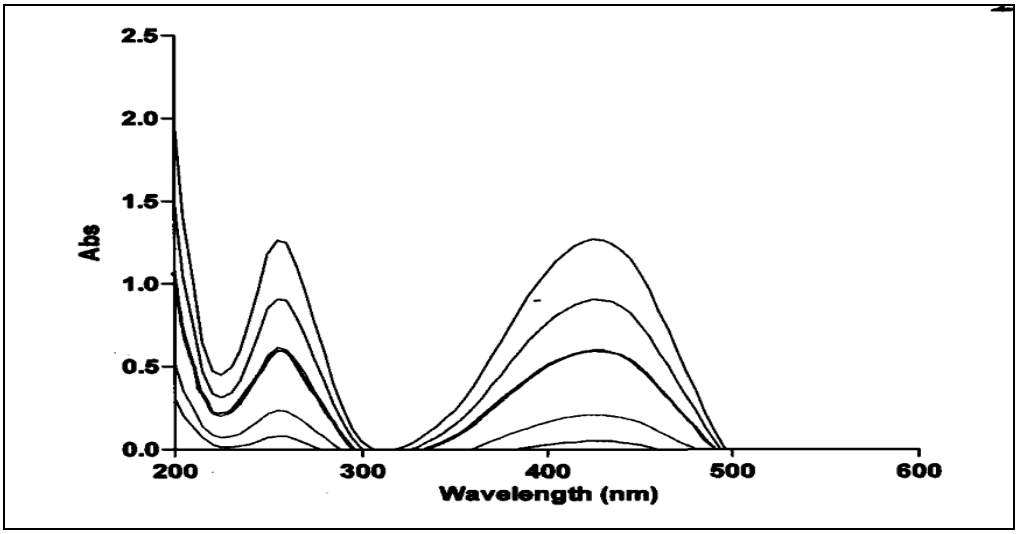

Figure 4 UV-Vis Spectrum of different concentration of Tartrazine

Military Technical College
Kobry El-Kobbah,
Cairo, Egypt

I.C.E.E.2016

8th International Conferenc
on
Chemical & Environmenta
Engineering
19 – 21 April 2016

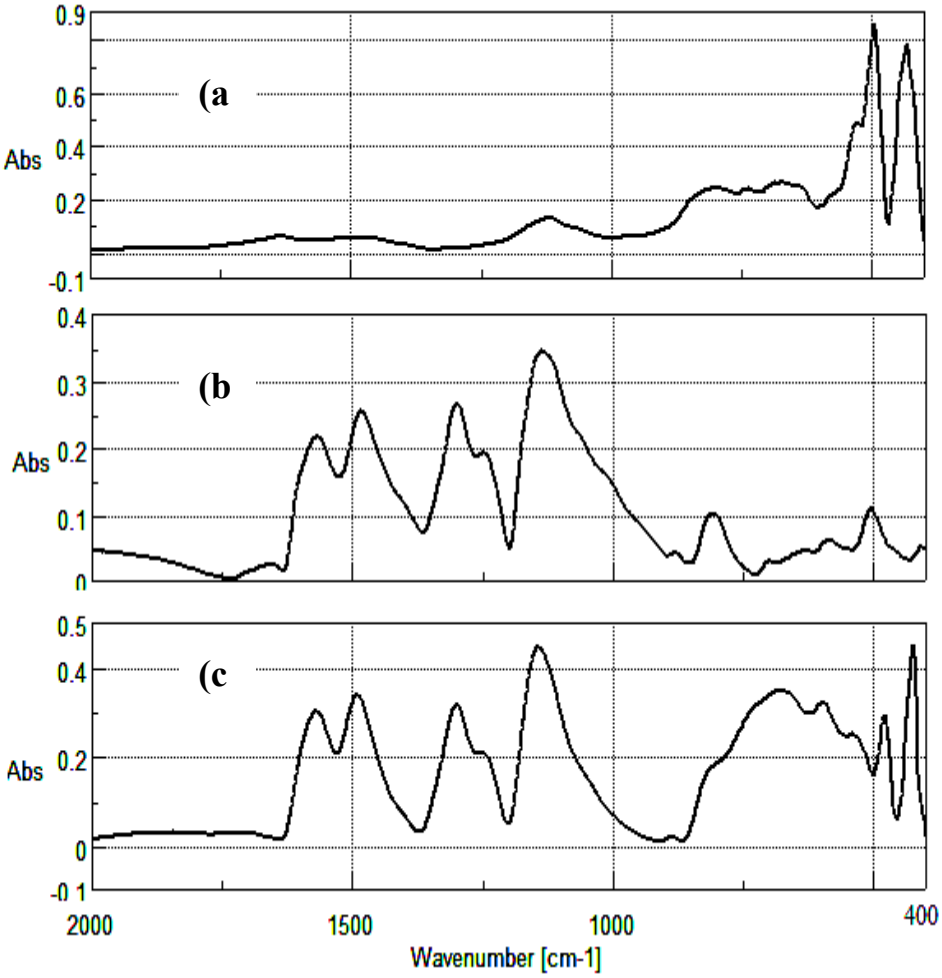

Figure 5. IR spectra of the prepared (a) TiO_2 (b) PANI (c) PT-1.

Military Technical College
Kobry El-Kobbah,
Cairo, Egypt

I.C.E.E.2016

8th International Conferenc
on
Chemical & Environmenta
Engineering
19 – 21 April 2016

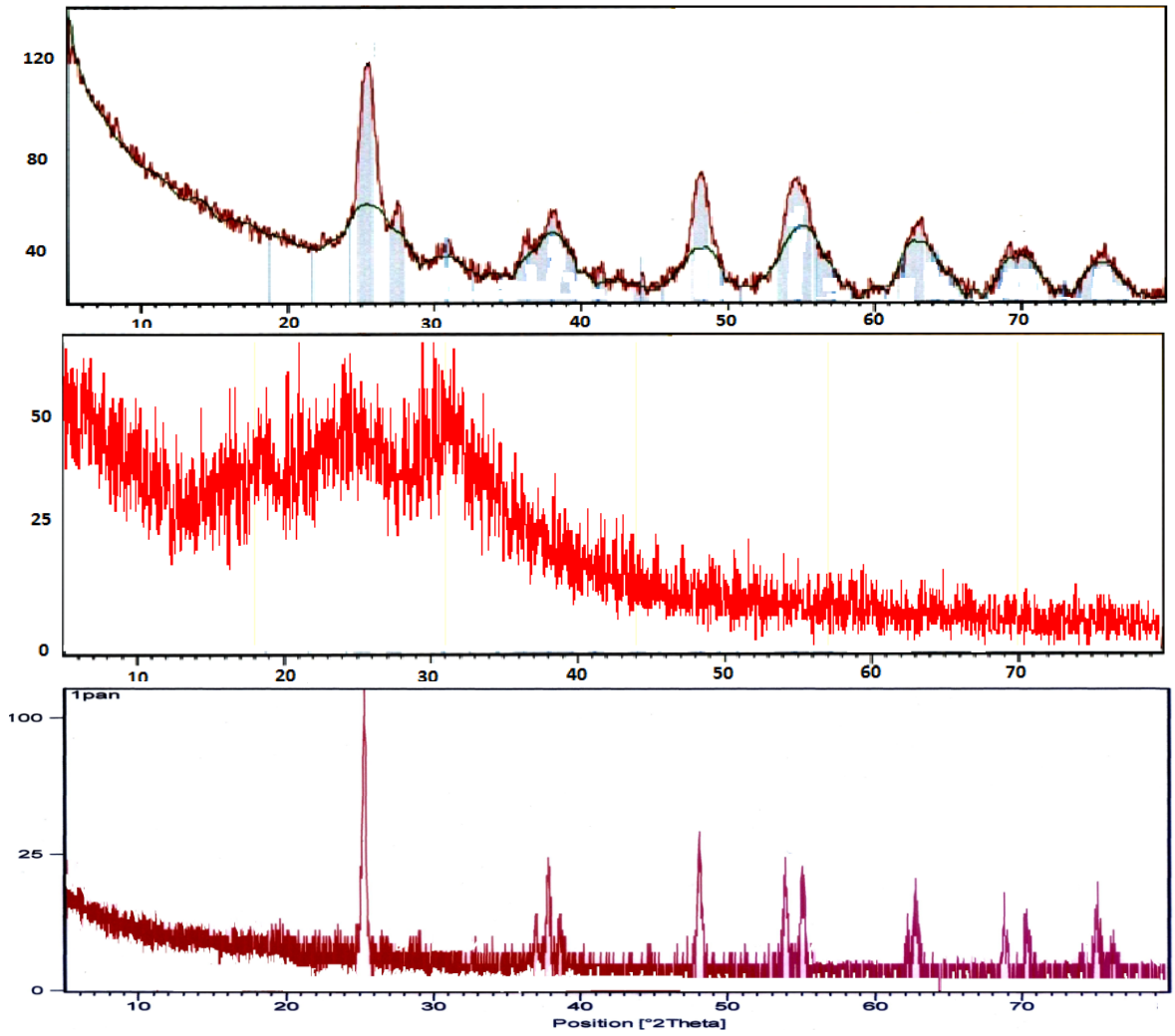

Figure 6. X-ray diffraction patterns of (a) the prepared TiO_2 (b) PANI and (c) PT-1 .

Military Technical College
Kobry El-Kobbah,
Cairo, Egypt

I.C.E.E.2016

8th International Conferenc
on
Chemical & Environmenta
Engineering
19 – 21 April 2016

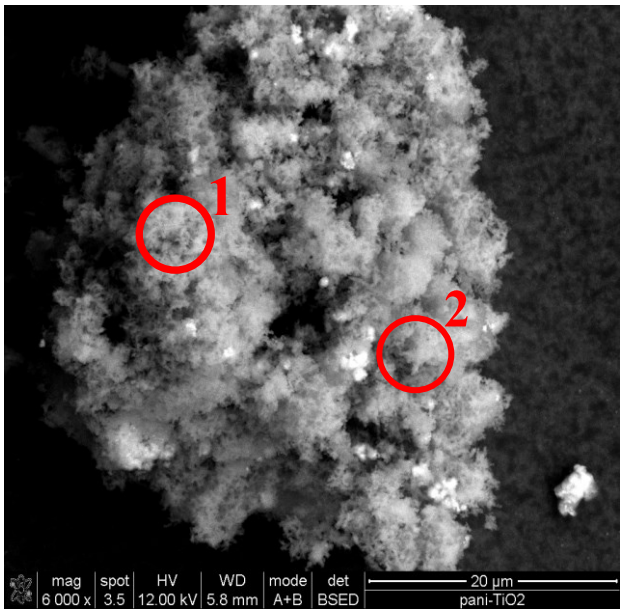

Figure 7. SEM image of PT-1 composite.

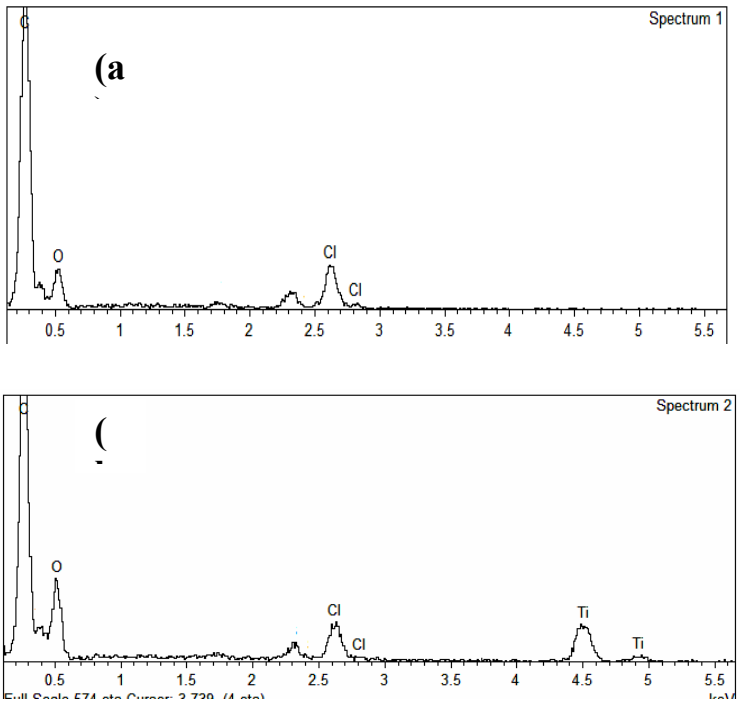

Figure 8. EDX spot analyses of points 1 and 2 in the SEM image

Military Technical College
Kobry El-Kobbah,
Cairo, Egypt

I.C.E.E.2016

8th International Conferenc
on
Chemical & Environmenta
Engineering
19 – 21 April 2016

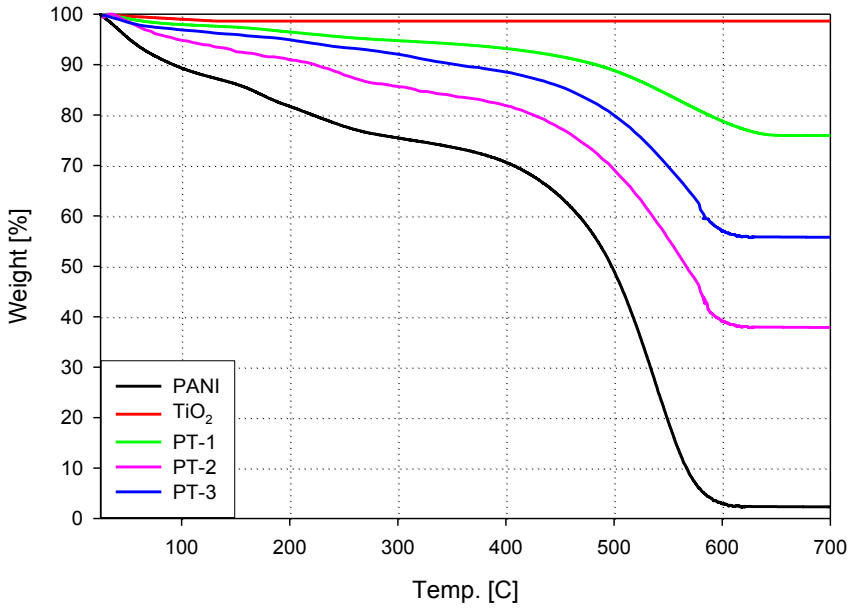

Figure 9 Thermal gravimetric analyses of PANI, TiO_2 and PT-1.

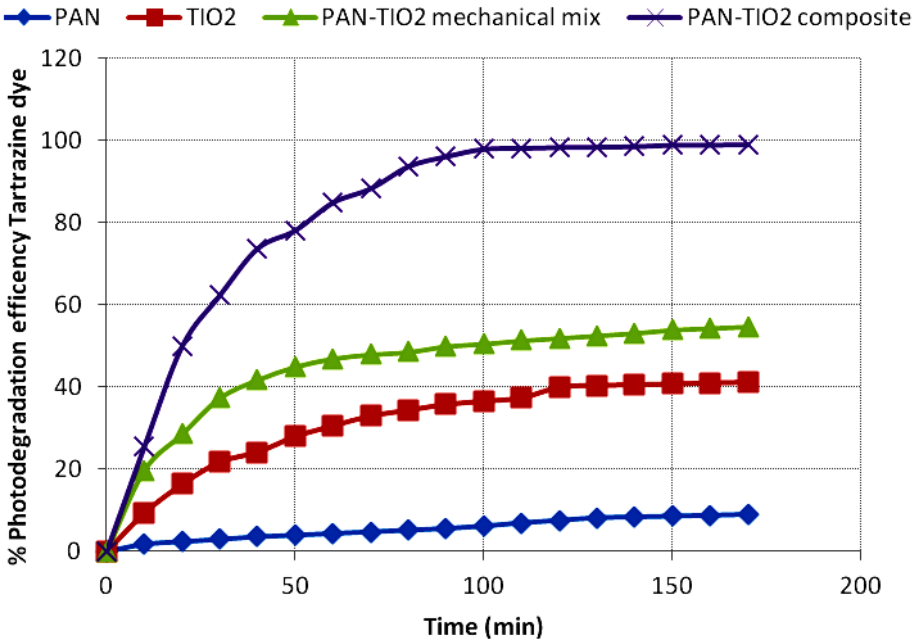

Figure 10. Degradation efficiency of TZ during 170 minutes by PANI, TiO_2, (PT-1) and (PT-mix) under UV-illumination.

Military Technical College
Kobry El-Kobbah,
Cairo, Egypt

8th International Conferenc
on
Chemical & Environmenta
Engineering
19 – 21 April 2016

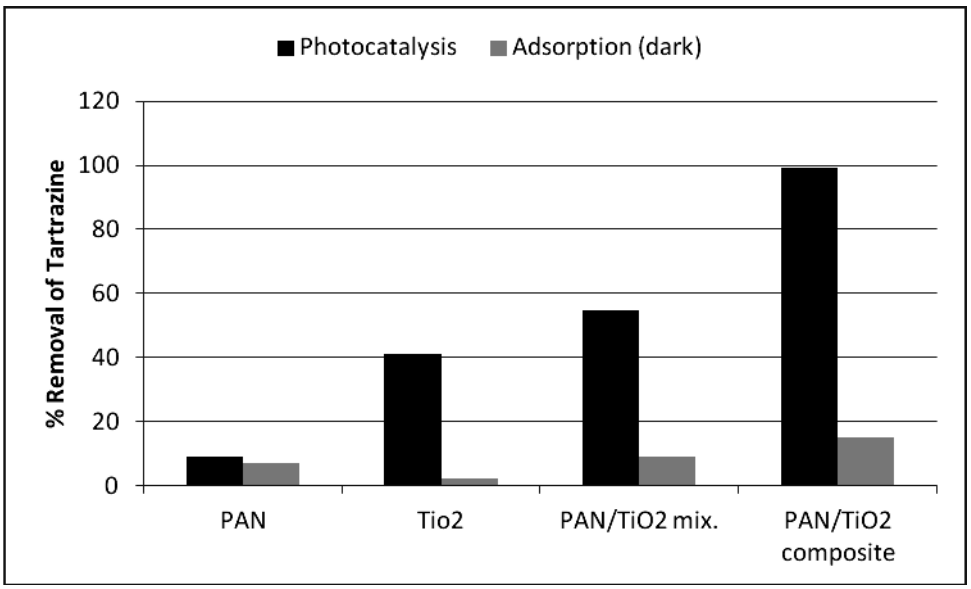

Figure 11. % Removal of Tatrazine dye (TZ) during 120 min with and without (dark) uv light using PAN, TiO_2, PT- mix and PT-1 composite samples

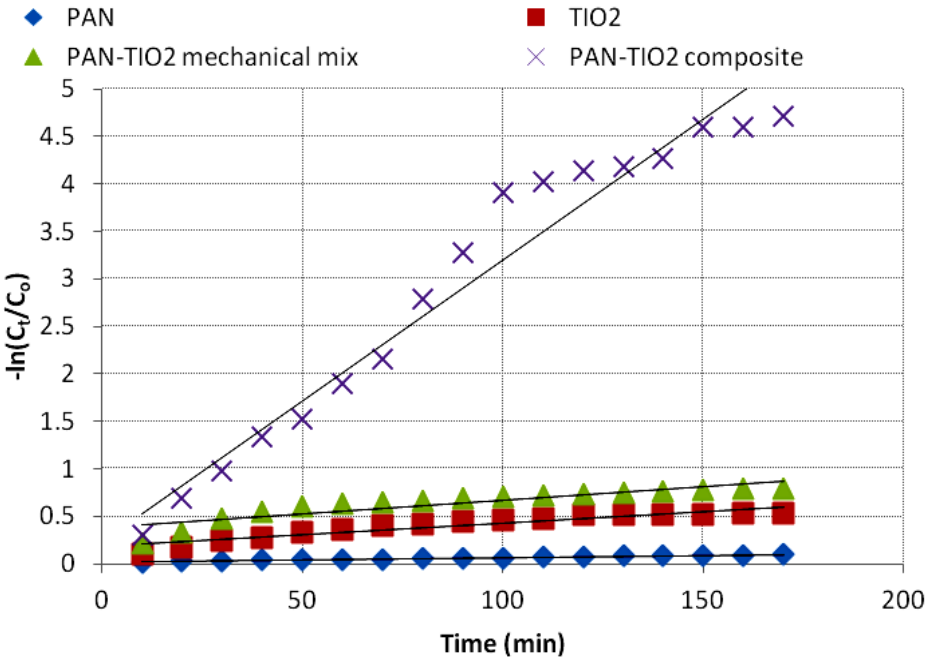

Figure 12 Kinetics plots for linear fitting of data obtained from pseudo-first-order reaction model for TZ degradation under UV light irradiation using PAN, TiO_2, PANI/TiO_2 mech. mix and PANI/TiO_2 composite(PT-1) as photo-catalyst.

Military Technical College
Kobry El-Kobbah,
Cairo, Egypt

I.C.E.E.2016

8th International Conferenc
on
Chemical & Environmenta
Engineering
19 – 21 April 2016

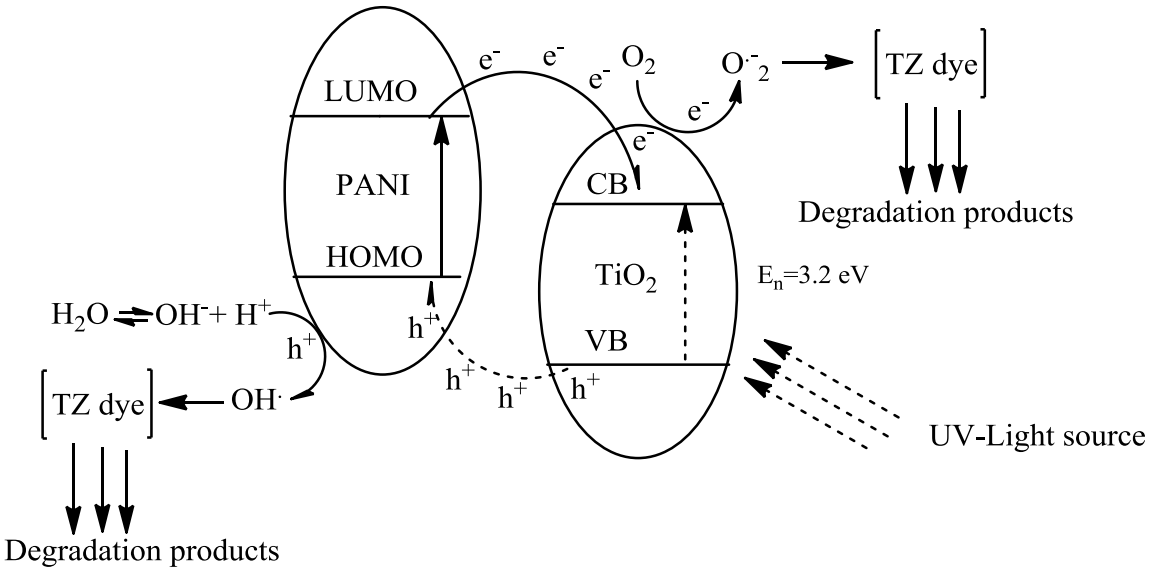

Figure 13 Mechanism of photo degradation of TZ dye by TiO_2/PANI photocatalyst under UV light irradiation

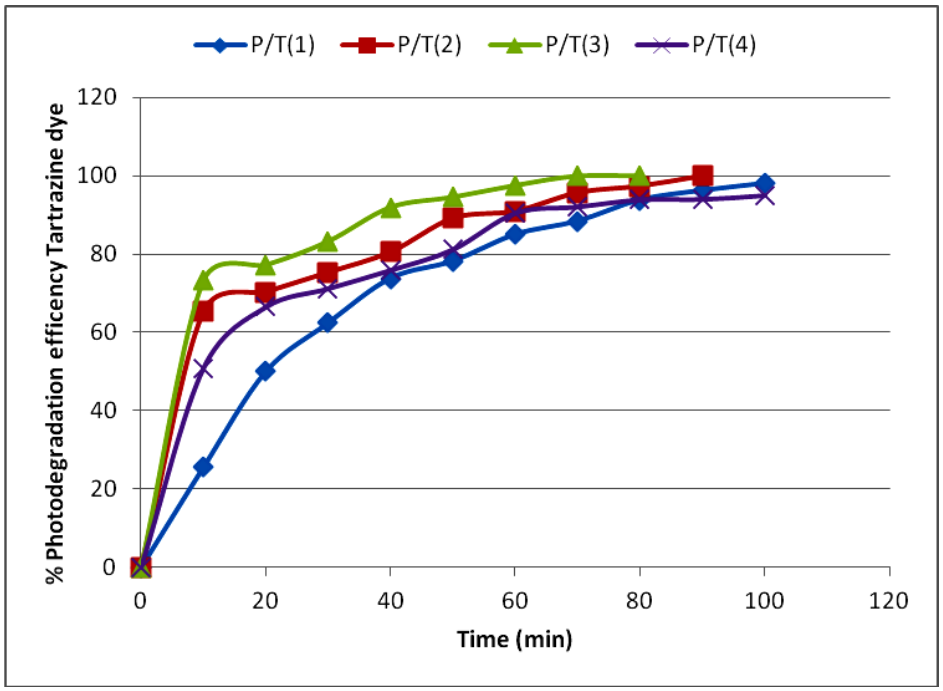

Figure 14 Effect of PANI/TiO_2 ratios on the degradation efficiency of TZ dye